Sensors and Materials, Vol. 34, No. 10 (2022) 3869–3881
MYU Tokyo

S & M 3082

Self-tuning Integral-type Finite-time-stabilized Sliding Mode Control for State Synchronization of Coronary Artery Systems

Chi-Hsin Yang,* Hao Ma, and Kun-Chieh Wang

School of Mechanical and Electric Engineering, Sanming University, Sanming 365004, Fujian Province, China

(Received July 4, 2022; accepted September 22, 2022)

Keywords: state synchronization, finite-time-stabilized, self-tuning sliding mode control, coronary artery system (CAS), voltage-sensing equipment

The medical treatment of cardiovascular disease can be regarded as synchronizing a chaotic diseased coronary artery system (CAS) to a healthy CAS in periodic motion. The main goal of the study is to develop a novel self-tuning integral-type finite-time-stabilized sliding mode control (IFSMC) scheme for two CASs with parameters belonging to different parameter sets to achieve their state synchronization. The defined integral-type finite-time-stabilized sliding mode (IFSM) has a special characteristic making it suitable for application to CASs. It is concluded that, on the sliding surface, one of the error states is first stabilized within a finite time. Then, the other error state becomes exponentially stable. The proposed adaptive IFSMC scheme contains four time-varying state feedback gains, which can adaptively compensate for the effects of nonlinear terms in the synchronized error dynamical system. Numerical simulations are performed to validate the effectiveness of the present scheme.

1. Introduction

Many medical experts have concluded that vasospasm is the main cause of myocardial ischemia and other cardiovascular diseases, such as common angina pectoris, sudden death, and myocardial infarction.(1) According to medical studies, vasospasm is caused by the behavior of blood vessels falling into chaotic states.(2) The coronary artery system (CAS)(3) mainly describes the dynamics of the changes in blood pressure in coronary artery vessels and in the inner radius of coronary artery vessels. Therefore, it is important to understand the nonlinear characteristics of the CAS and to suppress the occurrence of chaos in biomedical engineering.

Researchers have mainly investigated chaotic synchronization, which is the problem of tracking control between master–slave systems, to clarify the dynamical characteristics of nonlinear systems. Synchronization is the status of consistency with the time trajectories of state variables for master–slave systems.(4) The applications of chaotic synchronization, such as to the nervous system,(5) circuit systems,(6) secure communication,(7) encryption,(8) and micro-electro-mechanical systems,(9,10) have been paid considerable attention. From the viewpoint of biomedicine, a healthy CAS performs periodic motion and a diseased CAS performs chaotic

*Corresponding author: e-mail: 20190207@fjsmu.edu.cn
https://doi.org/10.18494/SAM4022

ISSN 0914-4935

motion. The medical treatment of cardiovascular disease can be regarded as synchronizing the chaotic cardiac behavior to that of a healthy CAS, so as to improve the pathology of a diseased CAS.[11]

Previous approaches for the chaotic synchronization of CASs include high-order sliding mode adaptive control,[1] where the effect of chatter was effectively alleviated by considering the unknown bound perturbation; the state feedback control scheme,[11] where the state equations of the CAS were equivalently transformed by differential transformation; the variable structure control scheme,[12] where the synchronized error system between two CASs was stabilized; the fuzzy logic control scheme,[13] where the cubic nonlinear term of the error dynamical system was directly eliminated by the applied state transformation; and terminal sliding mode control with adaptive rules,[14] where drive and response CASs were synchronized within a finite time. By considering the time delay in the CAS to design the control scheme for synchronization, finite-time synchronization with an input delay was proposed in Ref. 2, observer-based control schemes were addressed in Refs. 15 and 16, an H∞ synchronization approach was developed in Ref. 17, and an adaptive fuzzy control scheme was proposed in Ref. 18.

In practice, chaotic dynamical biological systems, such as a nerve-cell system and a CAS, can be realized by circuit implementation. For nerve-cell systems, hardware realizations by analog electronic circuits,[19,20] very large scale integration (VLSI),[21] and a field-programmable analog array[22] have been reported. For a CAS, the circuit realization and synchronization control of a cardiac system were studied in Ref. 23. Owing to its flexibility, real-time processing, and easy analysis, the analogy of a CAS with an electrical circuit is suitable for applications. Many voltage-sensing systems have been used to provide technologies for measuring the voltage in circuit systems.[24,25] The state variables of a CAS are analogized by the corresponding voltages in the circuits. Therefore, the time responses of an electrical CAS circuit for feedback control can be sensed by applying suitable voltage-sensing equipment. Furthermore, the control schemes developed for synchronization have also been applied in hardware circuit realization.[23]

Motivated by previous works,[1,12–14] in this study, the tracking control problem of state synchronization between master (healthy) and slave (disease) CASs is solved by introducing a novel self-tuning integral-type finite-time-stabilized sliding mode control (IFSMC) scheme. The novelty and main contributions of this study are listed below.

(1) The dynamical behavior of a chaotic CAS is mainly determined by the parameters of the system involved. In the literature,[12,13] two main parameter sets of chaotic CASs have been studied. In the previous works on state synchronization between two chaotic CASs, it was assumed that the two CASs were chaotic systems with parameters belonging to the same parameter set.[1,11–14,17,23] In this paper, the control problem of state synchronization between two chaotic CASs whose parameters belong to different parameter sets is discussed. Solving this control problem is not only more practically applicable but also more complicated.
(2) To solve the control problem of state synchronization between two CASs, an integral-type finite-time-stabilized sliding mode (IFSM) is defined. This sliding mode has a special stable characteristic. It is concluded that, on the sliding surface, one of the synchronized error states is first stabilized within a finite time, which is followed by the exponential stabilization of the other one. The proof of stability is given in detail.

(3) Using the defined sliding mode, a self-tuning IFSMC scheme for achieving state synchronization is developed. In past works on sliding mode control methods,[1,12,13] nonlinear terms, such as cubic items and external excitations, were directly eliminated by the equivalent control part. Different from the past works, the proposed self-tuning IFSMC scheme contains four time-varying state feedback gains, which can adaptively compensate for the effects of nonlinear terms in the synchronized error dynamical system. These time-varying feedback gains need not be decided in advance but are updated online according to specified rules. The stability of the overall closed-loop control system is also demonstrated.

The rest of this paper is organized as follows. The formulation of the control problem for state synchronization between two CASs is defined in Sect. 2. In Sect. 3, the design procedures of the self-tuning IFSMC scheme are developed. Furthermore, a proof of stability for the closed-loop control system is also provided. Numerical simulations are performed to validate the effectiveness of the proposed control scheme in Sect. 4. In Sect. 5, we make some final remarks.

2. Formulation of Control Problems for State Synchronization

The mathematical model of a CAS is described by the following nonlinear differential equations with respect to the normalized time t:[3,12]

$$\begin{cases} \dot{x}_1 = -bx_1 - cy_1 \\ \dot{y}_1 = -(\lambda + \lambda b)x_1 - (\lambda + \lambda c)y_1 + \lambda x_1^3 + E\cos(\sigma t) \end{cases}, \tag{1}$$

where the state variables x_1 and y_1 represent the changes in the normalized inner radius of the vessel and in normalized blood pressure in the vessel, respectively. The system parameters b, c, and λ dominate the behavior of the CAS. $E\cos(\sigma t)$ represents the external excitation factor acting on the blood vessels with amplitude E and frequency $f = \sigma/2\pi$. The bifurcation analysis of a CAS for different values of $E \in [0.1, 20]$ with system parameters $b = 0.15$, $c = -0.17$, $\lambda = -0.65$, and $\sigma = 1.0$ was discussed in Ref. 13. It was found that the CAS performs chaotic motion in the ranges of $0.3 \le E < 0.6$ and $4.5 \le E < 5.9$ and multi-periodic motion for other values of E.

In the study, the healthy master CAS is defined as a CAS in periodic motion. Figure 1 depicts the phase portrait for Eq. (1) with $\lambda = -0.65$, $E = 0.6$ without any control input; the CAS performs periodic motion.[13]

When a CAS performs chaotic motion, it is regarded to be diseased. Figure 2 depicts the phase portrait for Eq. (1) with $\lambda = -0.5$, $E = 0.3$ without any control input; the CAS descends into chaotic motion.[12] In this work, the diseased or slave CAS is built by the extension of the CAS shown in Fig. 2. Note that the CASs shown in Figs. 1 and 2 respectively belong to different parameter sets, as addressed in Refs. 12 and 13.

The model of the slave CAS is defined as

$$\begin{cases} \dot{x}_2 = -bx_2 - cy_2 \\ \dot{y}_2 = -(\lambda_s + \lambda_s b)x_2 - (\lambda_s + \lambda_s c)y_2 + \lambda_s x_2^3 \\ \qquad + E_s\cos(\sigma t) + \Delta(x_2, y_2) + d(t) + \mu(t) \end{cases}, \tag{2}$$

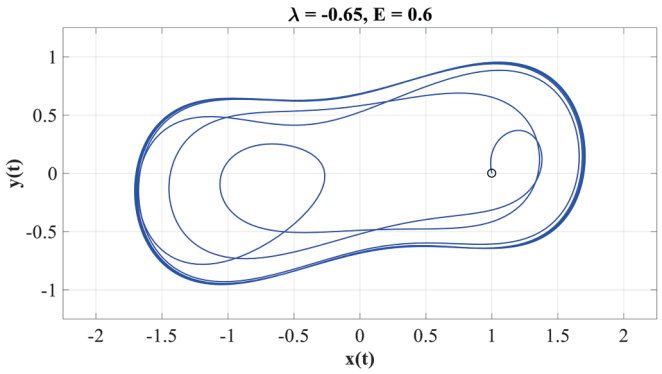

Fig. 1. (Color online) Phase portrait of healthy CAS (in periodic motion).

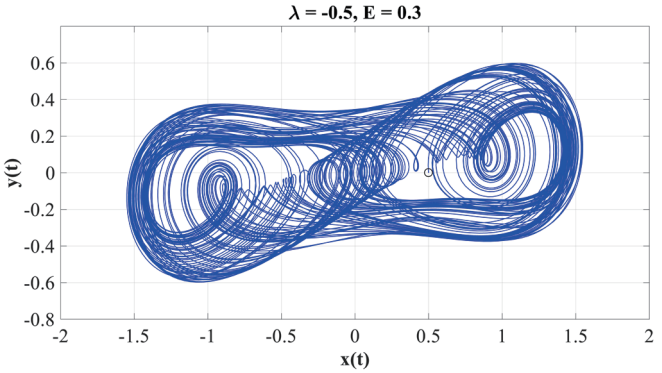

Fig. 2. (Color online) Phase portrait of diseased CAS (in chaotic motion).

where x_2 and y_2 are state variables. The system parameters λ_s and E_s are not equal to λ and E, which are applied to the healthy CAS in Eq. (1). $\Delta(x_2, y_2)$ and $d(t)$ are the unmodeled dynamics and another external disturbance, respectively. The designed control input $\mu(t)$, which is regarded as the potency or dosage of the medicine used for the treatment of angina and other heart disease,[12] is also included in Eq. (2).

The tracking control problem considered in this study is to develop an appropriate control scheme $\mu(t)$ such that the state variables of the slave CAS in Eq. (2) can synchronize with the master CAS in Eq. (1). That is, $\lim_{t\to\infty} x_2(t) \to x_1(t)$ and $\lim_{t\to\infty} y_2(t) \to y_1(t)$ for all given initial conditions. Such tracking control through a suitable therapy would enable a diseased CAS to become healthy.

Assumption

It is assumed that the uncertainty term $\Delta(x_2, y_2)$ and the other external disturbance $d(t)$ are unknown but bounded, that is,

$$0 < \left|\Delta(x_2, y_2)\right| < A_1, \quad 0 < \left|d(t)\right| < A_2. \tag{3}$$

The synchronized error states between the master and slave CASs in Eqs. (1) and (2) are defined by

$$e_x(t) = x_2(t) - x_1(t), \quad e_y(t) = y_2(t) - y_1(t). \tag{4}$$

By taking the derivative of Eq. (4) with respect to the normalized time t and substituting the CASs in Eqs. (1) and (2) into the derived results, the dynamical system of the synchronized error states for state synchronization is given by

$$\begin{cases} \dot{e}_x = -be_x - ce_y \\ \dot{e}_y = \lambda_s(F_1(x_1, x_2) - 1 - b)e_x - \lambda_s(1+c)e_y + (\lambda - \lambda_s)F_2(x_1, y_1), \\ \qquad + (E_s - E)\cos(\sigma t) + \Delta(x_2, y_2) + d(t) + \mu(t) \end{cases} \tag{5}$$

where $F_1(x_1, x_2) = x_1^2 + x_1x_2 + x_2^2$ and $F_2(x_1, y_1) = (1 + b)x_1 + (1 + c)y_1 - x_1^3$ are nonlinear and bounded functions. Because both the master and slave CASs are in chaotic or periodic motion, they are depicted as bounded phase portraits. In the design procedure of the control, $F_1(x_1, x_2)$ and $F_2(x_1, y_1)$ are assumed to have upper bounds and satisfy

$$0 < \left|F_1(x_1, x_2)\right| < B_1, \quad 0 < \left|F_2(x_1, y_1)\right| < B_2. \tag{6}$$

They are treated as time-varying coefficients of the synchronized error state $e_x(t)$ and the additional external disturbance, respectively. They are the key points to be resolved.

In this stage, the tracking control problem is equivalently transformed to stabilize the dynamical system in Eq. (5). The key point of the present control problem is to develop the control $\mu(t)$ such that the error states in Eq. (5) can tend to zero, that is, $\lim_{t\to\infty}\left|e_x(t)\right| \to 0$, $\lim_{t\to\infty} e_x(t) \to 0$, and $\lim_{t\to\infty}\left|e_y(t)\right| \to 0$. This is equivalent to the completion of state synchronization between the master and slave CASs in Eqs. (1) and (2).

Remark 1

In the previous works on state synchronization between two chaotic CASs, it was assumed that the two CASs had parameters belonging to the same parameter set for a chaotic system.[1,11–14,17,23] There are two parameter sets for chaotic CASs in the literature,[12,13] which must be included in the aforementioned formulation of the control problem.

3. Design of Novel Self-tuning Sliding Mode Control Scheme

In this study, we introduce a self-tuning IFSMC approach to achieve state synchronization between the CASs in Eqs. (1) and (2). The design approach of the self-tuning IFSMC scheme involves two basic steps. First, the novel integral-type finite-time stabilized sliding mode for the

desired sliding motion is selected. The defined sliding mode has special stable characteristics, for which we prove that, on the sliding surface, the synchronized error state $e_y(t)$ is first stabilized in a finite time, then the synchronized error state $e_x(t)$ is exponentially stabilized. Second, a robust and adaptive control $\mu(t)$ is designed, and it brings any state trajectory in the phase plane of the dynamical system in Eq. (5) to the sliding surface, where it remains, despite the presence of system uncertainties and external disturbances.

The IFSM $s(t)$ is defined by

$$s(t) = [e_y(t)]^{p/q} + \frac{1}{\rho}\left[e_x(t) + b\int_{\tau=0}^{\tau=t} e_x(\tau)d\tau \right], \tag{7}$$

where $\rho > 0$ and p, q are positive and odd integers with $1 < p/q < 2$ to avoid the singularity of the equivalent control. Theorem 1 provides a criterion guaranteeing the finite-time stability of $s(t) = 0$.

Theorem 1

For the IFSM $s(t)$ defined in Eq. (7) with the first equation in Eq. (5), the global finite-time stability of $e_y(t)$ is guaranteed for $s(t) = 0$ associated with $\dot{s}(t) = 0$. First, $e_y(t) \to 0$ is achieved in a finite time given by

$$T_s = \frac{\rho p}{|c|(p-q)}\left[e_y(t_0) \right]^{(p-q)/q} + t_0. \tag{8}$$

Then, it remains on $e_y(t) = 0\ \forall\ t \geq T_s > 0$, where $t = t_0 > 0$ is the time of the state trajectory $e_x(t)$, $e_y(t)$ in the phase plane from the initial values $e_x(0)$, $e_y(0)$ when it arrives at the sliding surface $s(t) = 0$. Subsequently, $e_x(t)$ is stabilized exponentially.

Proof

When the state trajectory $e_x(t)$, $e_y(t)$ is controlled to reach the sliding surface $s(t) = 0$ and remain there, $\dot{s}(t) = 0$ is also satisfied. The system dynamics is equivalent to the following nonlinear differential equation, obtained by substituting the first equation in Eq. (5) into $\dot{s}(t) = 0$:

$$\begin{aligned} &\dot{s}(t) = \frac{p}{q}\left[e_y(t) \right]^{p/q-1} \dot{e}_y(t) + \frac{1}{\rho}\left[\dot{e}_x(t) + be_x(t) \right] = 0 \\ &\Rightarrow \frac{de_y(t)}{dt} + \frac{(-c)q}{\rho p}\left[e_y(t) \right]^{2-p/q} = 0. \end{aligned} \tag{9}$$

Integrating with respect to the normalized time $t \in [t_0, t]$, where $t_0 > 0$ is defined as above, yields

$$\frac{q}{p-q}\left(\left[e_y(t)\right]^{p/q-1}-\left[e_y(t_0)\right]^{p/q-1}\right)=\frac{cq}{\rho p}(t-t_0). \tag{10}$$

The finite time T_s required to travel from $e_y(t_0) \neq 0$ to $e_y(T_s) = 0$ is given by

$$T_s=\frac{\rho p}{c(q-p)}\left[e_y(t_0)\right]^{p/q-1}+t_0, \quad c<0. \tag{11}$$

For the first equation in Eq. (5), it is obvious that the exponential stability of $e_x(t)$ is guaranteed by $b > 0$ and $e_y(t)=0, \forall t \geq T_s$ on the sliding surface $s(t) = 0$ associated with $\dot{s}(t)=0$. That is,

$$\dot{e}_x(t)+be_x(t)=0 \Rightarrow e_x(t)=e_x(T_s)\exp(-bt), \ \forall t \geq T_s, \tag{12}$$

thus completing the proof of Theorem 1.

Next, the robust and self-tuning IFSMC scheme $\mu(t)$ of the system in Eq. (5) for achieving state synchronization is introduced in Theorem 2.

Theorem 2

If $\mu(t)$ in Eq. (5) is taken to be the adaptive IFSMC scheme $\mu(t) = \mu_{eq}(t) + \mu_{sw}(t)$ with

$$\begin{aligned}
&\mu_{eq}(t)=\frac{cq}{\rho p}\left[e_y(t)\right]^{2-p/q},\\
&\mu_{sw}(t)=-\left[g_0(t)+g_1(t)\left|e_x(t)\right|+g_2(t)\left|e_y(t)\right|+g_3(t)\left|s(t)\right|^n\right]\cdot\text{sign}(s(t)),
\end{aligned} \tag{13}$$

where the design parameter is $0 < n < 1$, the sliding mode $s(t)$ is defined in Eq. (7), sign(•) denotes the sign function, and the self-tuning feedback gains $g_i(t)$, $i = 0, 1, 2, 3$ are updated according to the following algorithms:

$$\begin{aligned}
&\dot{g}_0(t)=\alpha_0\left|e_y(t)\right|^{p/q-1}\left|s(t)\right|, \quad g_0(0)=0, \alpha_0>0,\\
&\dot{g}_1(t)=\alpha_1\left|e_x(t)\right|\left|e_y(t)\right|^{p/q-1}\left|s(t)\right|, \quad g_1(0)=0, \alpha_1>0,\\
&\dot{g}_2(t)=\alpha_2\left|e_y(t)\right|^{p/q}\left|s(t)\right|, \quad g_2(0)=0, \alpha_2>0,\\
&\dot{g}_3(t)=\alpha_3\left|e_y(t)\right|^{p/q-1}\left|s(t)\right|^{n+1}, \quad g_3(0)=0, \alpha_3>0,
\end{aligned} \tag{14}$$

then the state trajectory $e_x(t)$, $e_y(t)$ in Eq. (5) asymptotically approaches the sliding surface $s(t) = 0$ and remains on it, i.e., $\dot{s}(t)=0$. It follows that $e_y(t)$ first tends to zero in a finite time T_s

evaluated using Eq. (8). Then, $e_x(t)$ is exponentially stabilized, thus accomplishing the state synchronization of the CASs in Eqs. (1) and (2).

Proof

The positive candidate Lyapunov function of the system in Eq. (5) is chosen as

$$V(t) = \frac{1}{2}s^2(t) + \frac{p}{2q}\sum_{i=0}^{3}\frac{(g_i(t)-K_i)^2}{\alpha_i} \geq 0, \tag{15}$$

where $K_i > 0$, $i = 0, 1, 2, 3$ are positive constants satisfying

$$\begin{aligned} &K_0 > \left(|\lambda| + |\lambda_s|\right)B_2 + E_s + E + A_1 + A_2, \\ &K_1 > |\lambda_s|(B_1 + 1 + b), \\ &K_2 > |\lambda_s|\left(1 + \left(|c|\right)\right), \\ &K_3 > 0. \end{aligned} \tag{16}$$

Taking the derivative of Eq. (15) with respect to t and substituting Eqs. (5), (7), (13), and (14) into the derived results, we obtain

$$\begin{aligned} \dot{V}(t) &= s(t)\dot{s}(t) + \frac{p}{q}\sum_{i=0}^{3}\frac{1}{\alpha_i}(g_i(t)-K_i)\dot{g}_i(t) \\ &= s\left[\frac{p}{q}(e_y)^{p/q-1}\dot{e}_y + \frac{1}{\rho}\left(\dot{e}_x + be_x\right)\right] + \frac{p}{q}\sum_{i=0}^{3}\frac{g_i(t)-K_i}{\alpha_i}\dot{g}_i(t) \\ \Rightarrow \dot{V}(t) &= s\frac{p}{q}(e_y)^{p/q-1}\cdot\Big[\lambda_s\left(F_1 - 1 - b\right)e_x - \lambda_s\left(1+c\right)e_y \\ &\quad + (\lambda - \lambda_s)F_2 + (E_s - E)\cos(\sigma t) + \Delta + d(t) \\ &\quad - \left(g_0(t) + g_1(t)|e_x| + g_2(t)|e_y| + g_3(t)|s|^{n+1}\right)\cdot \mathrm{sign}(s)\Big] \\ &\quad + \frac{p}{q}\sum_{i=0}^{3}\frac{g_i(t)-K_i}{\alpha_i}\dot{g}_i(t), \end{aligned} \tag{17}$$

$$\begin{aligned} \Rightarrow \dot{V}(t) \leq \frac{p}{q}|e_y|^{p/q-1}|s|\cdot\Big[&-\left(K_0 - \left(|\lambda| + |\lambda_s|\right)B_2 - E_s - E - A_1 - A_2\right) \\ &-\left(K_1 - |\lambda_s|\left(B_1 + 1 + b\right)\right)|e_x| - \left(K_2 - |\lambda_s|(1+|c|)\right)|e_y| - K_3|s|^n\Big] < 0. \end{aligned} \tag{18}$$

It is proved that $V(t)$ is a positive definite function from Eq. (15) and a decreasing function with respect to t from Eqs. (16) and (18). It follows that zero equilibria [$s = 0$, $g_i(t) = K_i$, $i = 0, 1, 2, 3$] are globally and asymptotically stabilized. This means that the state trajectory $e_x(t)$,

$e_y(t)$ in Eq. (5) asymptotically converges to $s(t) = 0$ with $\dot{s}(t) = 0$ from the given initial conditions $e_x(0)$, $e_y(0)$ when the self-tuning IFSMC scheme given by Eqs. (13) and (14) is applied.

On the sliding surface $s(t) = 0$, $e_y(t)$ is stabilized within a finite time T_s, which is evaluated using Eq. (8) with a suitable choice of $\rho > 0$ and positive and odd integers p and q with $1 < p/q < 2$. Then, according to Theorem 1, the exponential stabilization of $e_x(t)$ is guaranteed. Therefore, the synchronization between the two CASs in Eqs. (1) and (2) is accomplished, completing the proof.

Remark 2

The synchronized error state $e_x(t)$ in Eq. (5) is compensated adaptively without applying the equivalent control $\mu_{eq}(t)$ in Eq. (13).

Remark 3

The control scheme in Eq. (13) includes discontinuous control to reduce the amount of chatter, and the sign function in Eq. (13) is altered by $\tanh(s/\delta)$, where $\delta = 10^{-4}$ is a sufficiently small constant. The alteration is applied to the overall numerical simulation.

4. Numerical Simulations

Numerical simulations are performed to validate the effectiveness of the developed self-tuning IFSMC scheme. The fourth-order Runge-Kutta method with a time step size of 0.0001 and initial conditions $(x_1(0), y_1(0)) = (1.0, 0)$, $(x_2(0), y_2(0)) = (0.2, 0.2)$ is applied. Different from past studies,[1,12–14] the system parameters λ_s and E_s of the diseased CAS in Eq. (2) are not equal to λ and E of the healthy CAS in Eq. (1). The related simulation parameters for the numerical simulations are listed in Table 1.

The time histories of the master and slave CASs without control are depicted in Figs. 3 and 4, respectively. The numerical simulations are set up such that the master and slave CASs run individually without control from the initial conditions at $t = 0$. Then, the control input of the slave CAS is triggered to begin the process of state synchronization at $t = 10$. We show that by applying the proposed self-tuning IFSMC scheme, the slave (diseased) CAS undergoing chaotic motion can track the master (healthy) CAS undergoing periodic motion.

Table 1
Simulation parameters used in coding.

Parameter	Values
CAS parameters (common)	$b = 0.15$, $c = -1.7$, $\sigma = 1.0$
Master (healthy) CAS parameters	$\lambda = -0.65$, $E = 0.6$
Slave (diseased) CAS parameters	$\lambda_s = -0.5$, $E_s = 0.3$
Unmodeled dynamics	$\Delta(x_2, y_2) = 0.1\sin(x_2)\sin(y_2)$
External disturbance	$d(t) = 0.1\cos(2\sigma t)$
Designed parameters of control scheme	$p = 9$, $q = 7$, $\rho = 40$, $\alpha_0 = 15$, $\alpha_1 = 16$, $\alpha_2 = 12.5$, $\alpha_3 = 20$

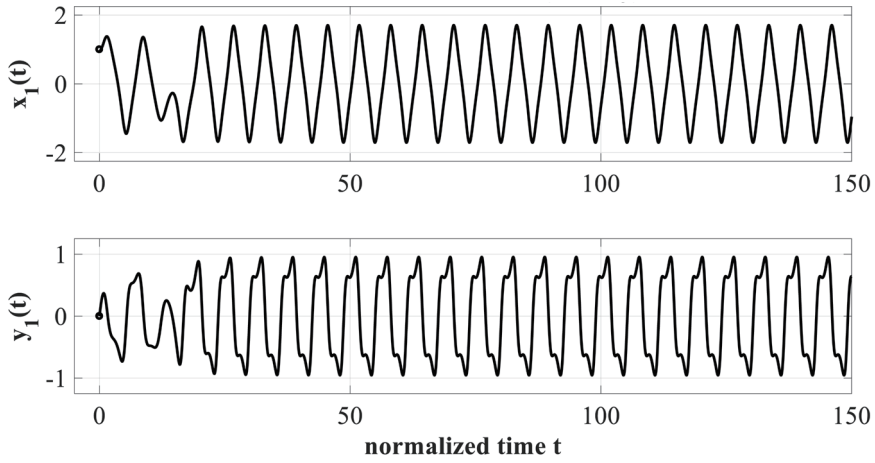

Fig. 3. Time histories of the master (healthy) CAS.

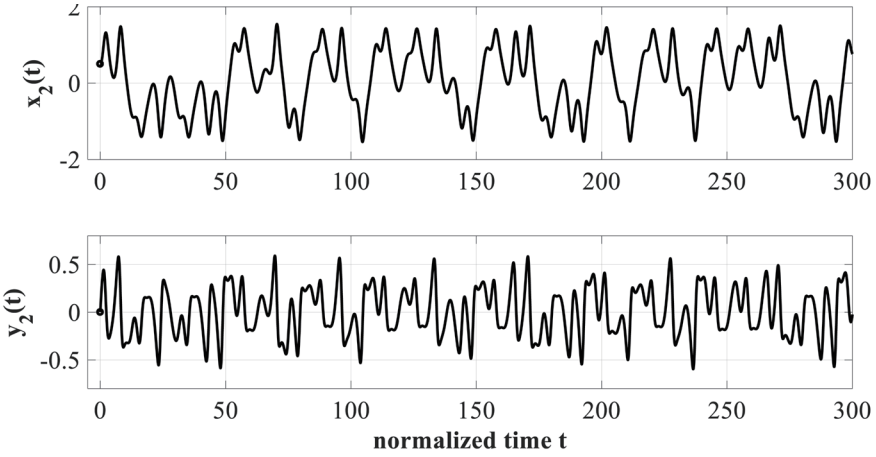

Fig. 4. Time histories of the slave (diseased) CAS.

The time responses of $e_x(t)$ and $e_y(t)$, and $s(t)$ are shown in Figs. 5 and 6, respectively. The figures show that $e_x(t)$, $e_y(t)$, and $s(t)$ oscillate irregularly when the control input is switched off, but when the control is applied at t = 10, $e_x(t)$, $e_y(t)$, and $s(t)$ converge to zero and state synchronization is achieved. Figure 6 shows that the control signal $\mu(t)$ is continuous and chatter-free. The time responses of $g_i(t)$, i = 0, 1, 2, 3 are shown in Fig. 7, where it can be seen that the gains become constant. The results indicate that $e_x(t)$ and $e_y(t)$, and the sliding mode $s(t)$ all tend to zero when the updating algorithms in Eq. (14) are applied.

Figure 8 displays the phase portrait of $e_x(t)$ and $e_y(t)$ from t = 0 to t = 50 in the phase plane. After the self-tuning IFSMC is triggered at t = 10, the state trajectory reaches $s(t)$ = 0 at t = 10.35, and $e_y(t)$ is first stabilized within a finite time. Then, $e_y(t)$ = 0 is maintained after t = 14.88 and $e_x(t)$ is subsequently exponentially stabilized. Finally, state synchronization is achieved. In Fig. 9, the time responses of the state variables for the master and slave CASs are exhibited. As expected, the state variables of the two CASs in Eqs. (1) and (2) separate from each other when different initial conditions are chosen. After the start of control at t = 10, the two state variables tend to synchronize despite the presence of system uncertainties and external disturbances.

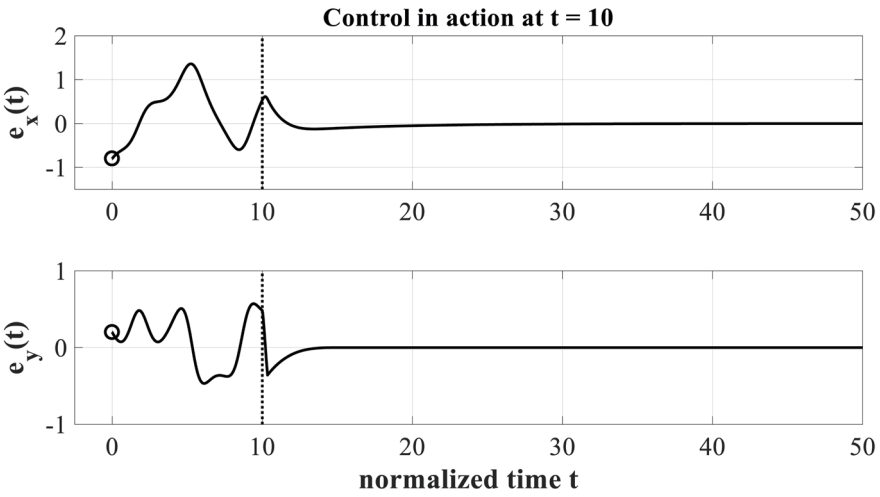

Fig. 5. Time responses of the synchronized error states $e_x(t)$ and $e_y(t)$.

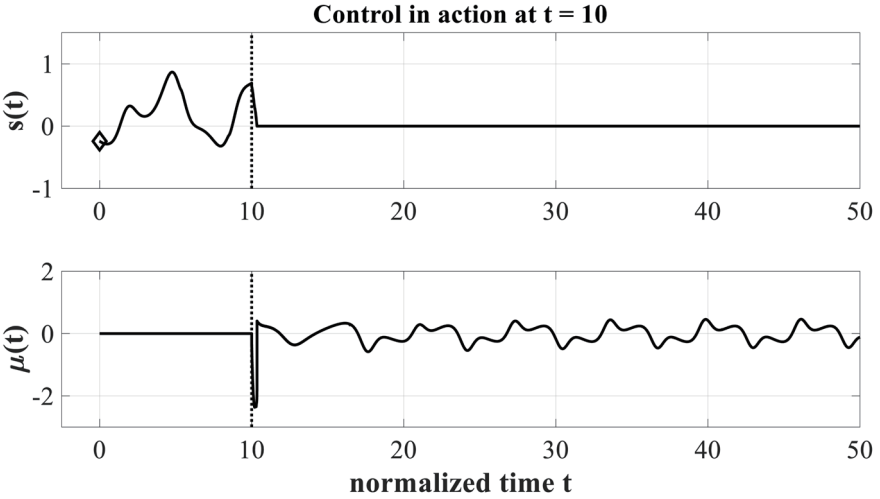

Fig. 6. Time responses of the sliding mode $s(t)$ and the control input $\mu(t)$.

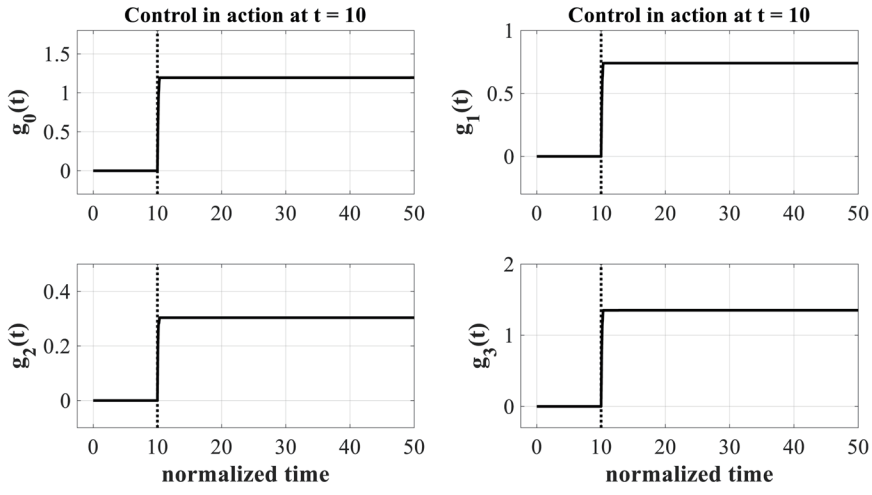

Fig. 7. Time responses of the adaptive feedback gains $g_i(t)$, $i = 0, 1, 2, 3$.

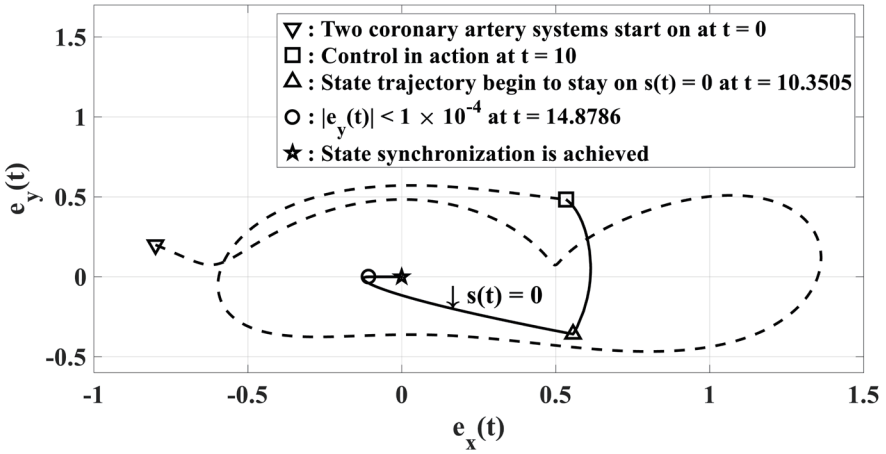

Fig. 8. Phase portraits of $e_x(t)$ and $e_y(t)$ from $t = 0$ to $t = 50$.

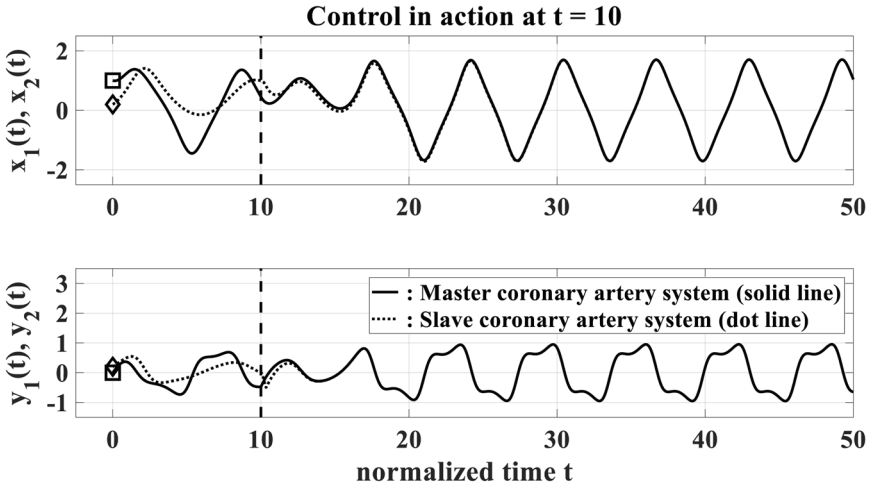

Fig. 9. Time responses of state variables for the master and slave CASs.

Compared with past works,[1,11–14,17,23] where the chaotic synchronization between two CASs with parameters in the same parameter set was studied, the present work shows that the state synchronization between two chaotic CASs with parameters belonging to different parameter sets can be achieved using the introduced scheme.

5. Conclusions

To solve the tracking control problem of state synchronization between master and slave CASs, the special property of the defined IFSM is proven. That is, the error state $e_y(t)$ is first stabilized within a finite time on the sliding surface $s(t) = 0$. Then, the error state $e_x(t)$ is exponentially stabilized. To achieve the control goal, the novel self-tuning IFSMC approach has been addressed and the stability of the closed-loop system is also guaranteed. Numerical simulations are performed to validate the effectiveness of the present control scheme. According

to a previous study,[23] the developed control scheme for synchronization can be implemented by hardware circuit realization. Our proposed scheme can be extended to the study of other control problems, such as projective or anti-synchronization, belonging to the field of the CAS in future works.

Acknowledgments

This work was supported by the Operational Funding of the Advanced Talents for Scientific Research (19YG04) of Sanming University, Sanming City, Fujian Province, China. We also acknowledge the School of Mechanical and Electrical Engineering of Sanming University.

References

1 Z. S. Zhao, J. Zhang, G. Ding, and D. K. Cheng: Acta Phy. Sin. **64** (2015) 210508. https://doi.org/10.7498/aps.64.210508
2 S. Harshavarthini, R. Sakthivel, and F. Kong: Chaos Solitons Fractals **134** (2020) 109683. https://doi.org/10.1016/j.chaos.2020.109683
3 Y. Shi: Discrete Dyn. Nat. Soc. **2012** (2012) 631476. https://doi.org/10.1155/2012/631476
4 L. M. Pecora and T. L. Carroll: Phys. Rev. Lett. **64** (1990) 821. https://doi.org/10.1063/1.4917383
5 C. C. Yang and C. L. Lin: Nonlinear Dyn. **69** (2012), 2089. https://doi.org/10.1007/s11071-012-0410-6
6 U. E. Kocamaz, B. Cevher, and Y. Uyaroglu: Chaos Solitons Fractals **105** (2017) 92. https://doi.org/10.1016/j.chaos.2017.10.008
7 Y. Z. Liu, Y. Y. Xie, Y. C. Ye, J. P. Zhang, S. J. Wang, Y. Liu, G. F. Pan, and J. L. Zhang: IEEE Photo. J. **9** (2017) 7900512. https://doi.org/10.1109/JPHOT.2016.2639291
8 Z. Wu, X. Zhang, and X. Zhong: IEEE Access **7** (2019) 37989. https://doi.org/10.1109/ACCESS.2019.2906770
9 H. Y. Chen, K. C. Wang, H. C. Shen, and C. H. Yang: Microsyst. Tech. **27** (2021) 1107. https://doi.org/10.1007/s00542-018-4088-7
10 C. H. Yang, K. C. Wang, and L. Wu: Sens. Mater. **32** (2020) 3343. https://doi.org/10.18494/SAM.2020.2918
11 W. S. Wu, Z. S. Zhao, J. Zhang, and L.K. Sun: Nonlinear Dyn. **87** (2017) 1773. https://doi.org/10.1007/s11071-016-3151-0
12 C. J. Lin, S. K. Yang, and H. T. Yau: Comput. Math. Appl. **64** (2012) 988. https://doi.org/10.1016/j.camwa.2012.03.007
13 C. C. Wang and T. Y. Her: Abstr. Appl. Anal. **2013** (2013) 209718. http://dx.doi.org/10.1155/2013/209718
14 Z. Zhao, X. Li, J. Zhang, and Y. Pei: Inter. J. Biomath. **10** (2017) 1750041. https://doi.org/10.1142/S1793524517500413
15 J. Guo, Z. S. Zhao, F. D. Shi, R. K. Wang, and S. Li: IEEE Access **7** (2019) 51222. https://doi.org/10.1109/ACCESS.2019.2909749
16 J. Guo and Z. S. Zhao: Modern Phy. Lett. B **33** (2019) 1950454. https://doi.org/0.1142/S0217984919504542
17 X. M. Li, Z. S. Zhao, J. Zhang, and L. K. Sun: Chin. Phys. B **25** (2016) 060504. https://doi.org/10.1088/1674-1056/25/6/060504
18 Z. Y. Zhu, Z. S. Zhao, J. Zhang, R. K. Wang, and Z. Li: Inf. Sci. **535** (2020) 225. https://doi.org/10.1016/j.ins.2020.05.056
19 A. Petrovas, S. Lisauskas, and A. Slepikas: Elec. Electr. Eng. Kaunas: Tech. **122** (2012) 117. https://doi.org/10.5755/j01.eee.122.6.1835
20 S. Binczak, S. Jacquir, J. M. Bilbault, V. B. Kazantsev, and V. I. Nekorkin: Neural Networks **19** (2005) 684. https://doi.org/10.1016/j.neunet.2005.07.011
21 J. Cosp, S. Binczak, J. Madrenas, and D. Fernandez: Inter. J. Elec. **101** (2014) 220. https://doi.org/10.1080/00207217.2013.780263
22 J. Zhao and Y. B. Kim: Proc. 2007 50th Midwest Symp. Circuits and Systems (MWSCAS, 2007) 772. https://doi.org/10.1109/MWSCAS.2007.4488691
23 C. Y. Yeh, J. Shiu, and H. T. Yau: Math. Prob. Eng. **2012** (2012) 745396. https://doi.org/10.1155/2012/745396
24 F. C. Pereira, J. H. Galeti, R. T. Higuti, M. J. Connelly, and C. Kitano: J. Lightwave Tech. **1** (2017) 3257. https://doi.org/10.1109/JLT.2018.2840706
25 Y. Hea, Q. Yang, S. Sun, M. Luo, R. Liu, and G. D. Peng: Int. J. Elec. Power Ener. Syst. **117** (2020) 105607. https://doi.org/10.1016/j.ijepes.2019.105607